

Coherence of the light of firefly *Luciola praeusta*

Upamanyu Sharma, Angana Goswami and
Anurup Gohain Barua*

Department of Physics, Gauhati University, Guwahati 781 014, India

Firefly bioluminescence has given rise to several curiosity-driven as well as application-oriented studies. The emission spectrum of the Indian species of firefly *Luciola praeusta* Kiesenwetter 1874 (Coleoptera: Lampyridae: Luciolinae) has been shown to consist of two broad green- and red-coloured sectors, with a narrow yellow one in between. Here we present interference patterns of light of this firefly species using a Michelson interferometer for different positions of the two reflecting mirrors, up to a path difference of 11.5 cm. Next we employ Young's double-slit method with the lantern of the firefly as the source at pinhole separations of 160, 170 and 180 μm . From the fringes obtained in these two sets of experiments, we conclude that the light of the firefly exhibits excellent temporal as well as good spatial coherence properties.

Keywords: Bioluminescence, firefly, interference patterns, temporal and spatial coherence.

THE process of conversion of chemical energy into light by living organisms is known as bioluminescence. Perhaps the best known example of bioluminescence is the method by which fireflies produce light. This reaction, also called chemiluminescent reaction, can be outlined in two steps¹. In the first step, luciferin is converted into a luciferyl adenylate by adenosine triphosphate (ATP) in the presence of magnesium ions. In the next step, luciferyl adenylate is oxidized by molecular oxygen resulting in the emission of light and production of oxy-luciferin. The reaction is efficient; its quantum yield value, recently determined to be 41%, is much higher than those of chemiluminescence and bioluminescence of other organisms². Spectral spreads of the light of different species of fireflies have been studied for over a century. Measurements of the full width at half maximum (FWHM) in the emission spectra of the Indian species *Luciola praeusta* have put the value at 55 nm, spreading from 537 to 592 nm (ref. 3). Emission spectra of this species on colour films have shown three colour sectors: green, yellow and red, spreading from about 490 to 580 nm (ref. 4). Recording double-slit interference and grating diffraction patterns of this species, it has been inferred that the firefly emission has a tendency for spectral narrowing within the narrow yellow sector of the spectrum^{4,5}. This conclusion has been arrived at due to the fact that the interference pattern produced in a double-slit demonstrated

predominance of the yellow sector, and the diffraction pattern produced in a grating showed the central principal diffraction maximum as yellow, which shrunk considerably in the other two maxima. It has been observed that the time-resolved spectrum in the microsecond scale of this species exhibited resemblance with the output of a multimode laser³. A striking finding in recent times has been the appearance of a narrow strong line at 591 nm in the emission spectrum of this species; it has been hypothesized that the emission of this line is akin to that of a random laser⁶. Very recently, the steady-state spectrum recorded for another Indian species, *Asymmetricata circumdata* in a high-resolution spectrometer has shown the peak wavelength at 570 nm, while the same on a colour film in a glass spectrograph revealed the peak at 579 nm between green and red bands, prompting speculation that a sharp line might exist in the emission spectrum of this species just as in the case of *L. praeusta*⁷.

Biologically derived or even biologically produced materials and structures have been attracting increasing attention for photonic applications. Optofluidic biolasers, which incorporate biochemical or biological molecules in the gain medium, have proved to be superior or equal to fluorescence-based bio-sensing. D-luciferin or firefly luciferin, among other biosynthesized materials, has been used as the gain medium in the demonstration of optofluidic lasers⁸. In this study, we examine the coherence properties of the 'laser-like' light from the firefly. Michelson interferometer and Young's double-slit have been the standard methods used to measure temporal and spatial properties of light respectively. Coherence length indicates the propagation length during the time in which the phase of the wave changes by a significant amount – reducing the interference, while spatial coherence indicates how far apart two sources, or two points of the same source, are in a direction perpendicular to the direction of propagation and still exhibit the interfering property. Surprisingly good values of coherence coming out in the firefly emission indicate the potential of construction of an efficient laser system.

Figures 1 and 2 show the experimental set-up for studies of temporal and spatial coherence respectively. Before the experiment, mirrors M1 and M2 in the two arms of the Michelson interferometer were adjusted to obtain the best possible interference fringes for zero path difference of the two beams. The interferometer was tested for a commercial multimode helium neon laser of wavelength 632.8 nm by varying the interferometer arms. Just prior to the experiment, a few male specimens from the campus of Gauhati University were caught. One of them was fitted with a beam expander such that radiation passing through a diffuser arrived at the beam splitter. At first, for recording the interference pattern for zero path difference, both M1 and M2 were placed at an optical distance of 12 cm from the beam splitter (at positions marked 8.5 cm in the scales on the arms of the interferometer).

*For correspondence. (e-mail: agohainbarua@yahoo.com)

Keeping M2 fixed, M1 was slowly moved in steps of 1 mm towards the beam splitter. Interference patterns were recorded in each step with a NIKON D7000 camera fitted with AF-S 50 mm NIKKOR f/1.4 G lens. When M1 reached the zero of the scale, which is at a distance of 3.5 cm from the beam splitter, it was kept fixed there and M2 in the other arm was gradually moved away from the beam splitter compensator in steps of 1 mm till the interference rings disappeared. The experiment was also performed without the diffuser to compare with and verify the result.

For spatial or transverse coherence, two pinholes of diameter 160 μm were made in a black paper board with a micro pin. In this experiment, the firefly was placed in a groove made in a black-coloured, thick sponge and fixed with cotton and Sellotape with its light organ facing the pinholes. The distance between the source and the plane of the holes was varied from 1 to 5 mm in order to obtain the best fringes. The fringes were produced with a gap of 3 mm between the firefly lantern and the two holes. The

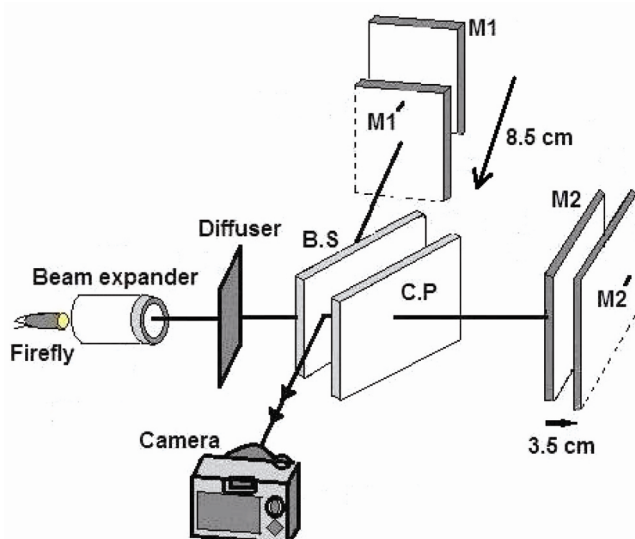


Figure 1. Schematic of the experimental set-up of the Michelson interferometer. The initial position of the movable mirror is at M1, which can be moved a maximum of 8.5 cm from that position towards the beam splitter (B.S.) to M1'; the other mirror M2 can be moved away from the compensating glass plate (C.P.) up to a maximum distance of 3.5 cm to M2'.

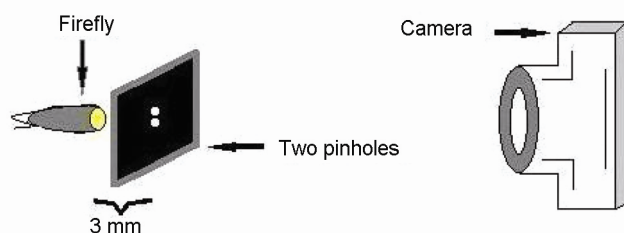


Figure 2. Arrangement for the double-slit experiment. Different separation pinholes are used for obtaining fringes of varying contrasts.

distance of the camera from the pinholes was about 30 cm. A closer view of the central fringe was also obtained. As done in the case of the Michelson interferometer, the double-slit experiment was also carried out for the laser source.

Thirty firefly specimens were used in the experiments. Intensity profiles were plotted using the software ImageJ, where a rectangular region was selected along the horizontal direction enclosing all the fringes from left to right. The experiments were performed in a dark room – a typical spectroscopy research laboratory free from ambient light interference/contamination – at a temperature of 27°C. The experiments could be easily reproduced, with this or other species of fireflies.

Using the firefly, when one of the mirrors in the Michelson interferometer is blocked, only a general illumination is visible (Figure 3). Figure 4a presents the interference pattern for an equal optical path length of the two mirrors in the Michelson interferometer. It is well known that interference fringes of best contrast are observed for zero path difference of the two interfering beams, and this figure represents the same. Yellow 'bright' rings are clear while the 'dark' spaces are not exactly dark: they are occupied by green and red colours. We regard emissions in green and red sectors as noise while those in the narrow yellow sector as the signal. It is clear that in spite of the effect of this 'noise', the bright rings are quite prominent, which could also be noticed in the intensity profile (Figure 4b). With increasing path difference, the contrast between bright and dark fringes becomes poorer. This is evident in Figure 5a–f for path differences of 2, 4, 6, 8, 10 and 11.5 cm respectively. Figure 6 shows somewhat better view of these fringes. In the present experiment, green and red colours fill up the dark spaces in a random fashion as bioluminescence intensity depends considerably on the angle of emission, and it is not possible to keep the surfaces of the light-emitting portions of the firefly exactly parallel or

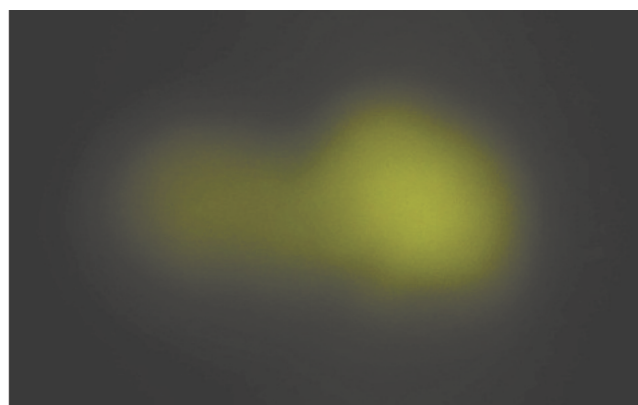


Figure 3. General illumination when one of the mirrors in the Michelson interferometer is blocked for zero optical path length difference in the two arms. No interference fringe is noticeable.

perpendicular to the mirrors M2 and M1 respectively. Hence as the optical path length changes in the interferometer arms, the received light intensity would depend on the fitted position or placement of the firefly; even at the same optical path length for different specimens, the value of the visibility function varies widely, and calculation of the visibility function could be considered as

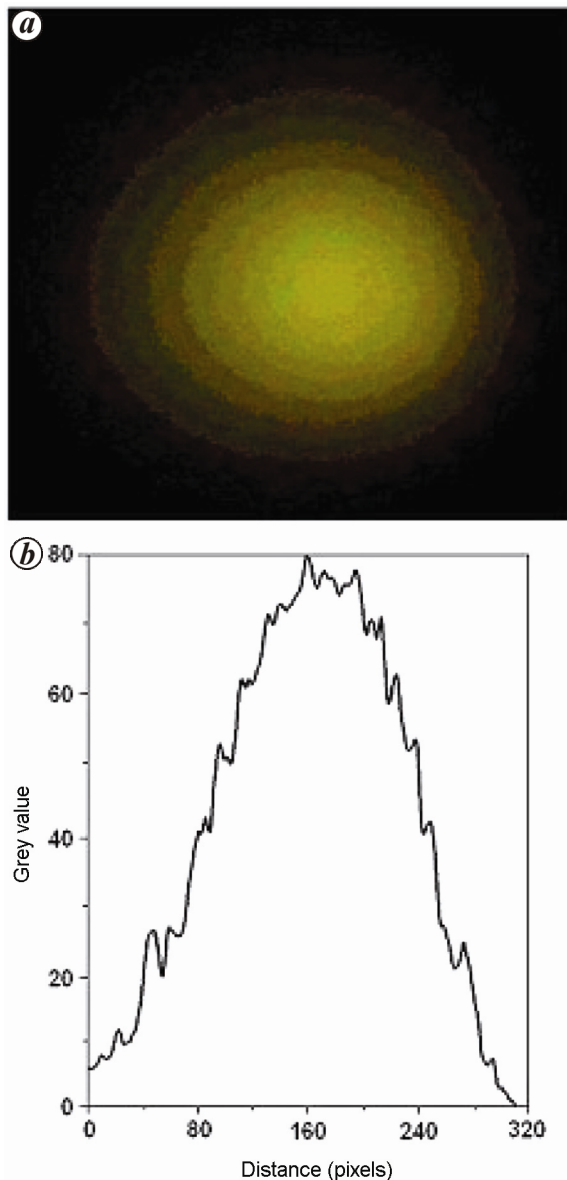


Figure 4. Interference pattern of the light of the firefly *Luciola praeusta* in a Michelson interferometer. **a**, For equal optical path lengths of the two mirrors. Rings come out as bright yellow, while dark spaces appear to be filled by green and red colours. As expected, fringes of best contrast are produced in this set-up. **b**, Oscillating intensity plot. Even though the ‘dark’ spaces are filled up by green and red colours, the maxima are easily noticeable, especially towards the lower intensity side away from the centre. A total of eight interference maxima, of which one is relatively weak, can be observed in this plot in each of the rising and falling halves. The central fringe in the middle shows the highest grey value. Here one pixel corresponds to a distance of $4.78 \mu\text{m}$.

pointless in the present experiment. Even with the use of a yellow filter (Edmund Optics, peak: 589 nm , FWHM: 10 nm) because of the presence of light apart from the sharp one at 591 nm , the visibility function fluctuates. This fact would remain even if one uses a narrower bandwidth filter, unless the peak of the filter is at the same position and FWHM has the same value as the narrow line. Still, to have an idea of the distribution of intensity, Figure 7 *a–f* presents intensity profiles of these interference patterns. Because of the diminishing contrast, two-point smoothing for Figure 7 *c* and *d*, three-point smoothing for Figure 7 *e*, and eight-point smoothing for Figure 7 *f* are done in Origin 6.0. The light-emitting

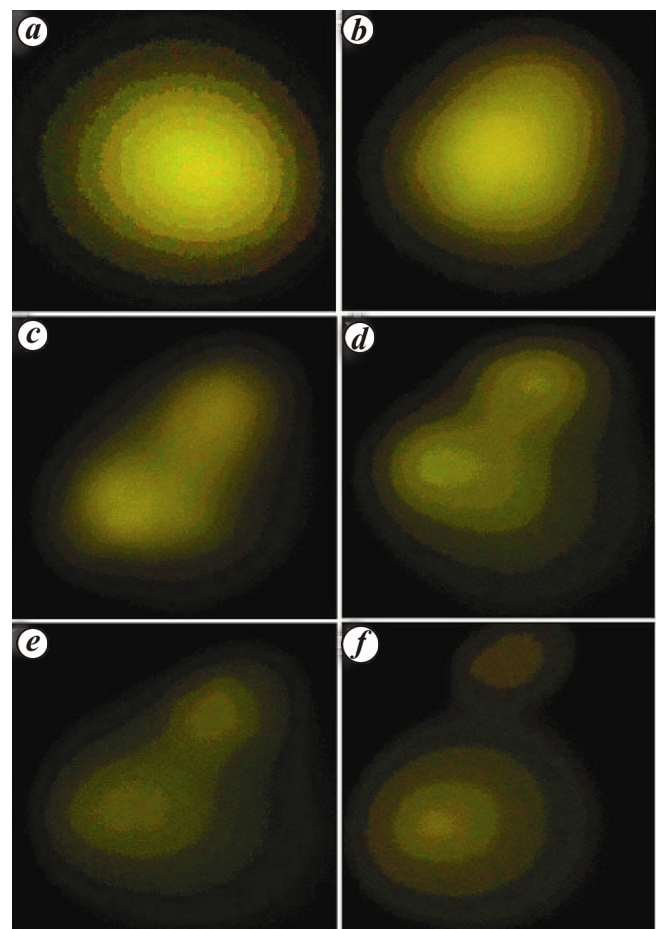


Figure 5. Interference patterns obtained in the Michelson interferometer for different positions of the mirrors. **a**, For a path difference of 2 cm : bright yellow rings, similar to those for no path difference, appear with dark regions occupied by green–red colours with slightly diminished contrast. **b**, For a path difference of 4 cm : the contrast gets more diminished. **c**, For a difference of 6 cm : fringes are about to manifest in the two images individually on moving one of the mirrors close to the beam splitter, while the envelope of the combined interference pattern produced by the two light-emitting segments of the firefly shows a lower contrast. **d**, For a path difference of 8 cm : fringes in the two images get clearer while the contrast of the combined interference pattern gets poorer. **e**, For a 10 cm difference: fringes show a poor appearance. **f**, For a difference of 11.5 cm : interference fringes produced by the two segment-sources disappear, but those belonging to the individual ones remain.

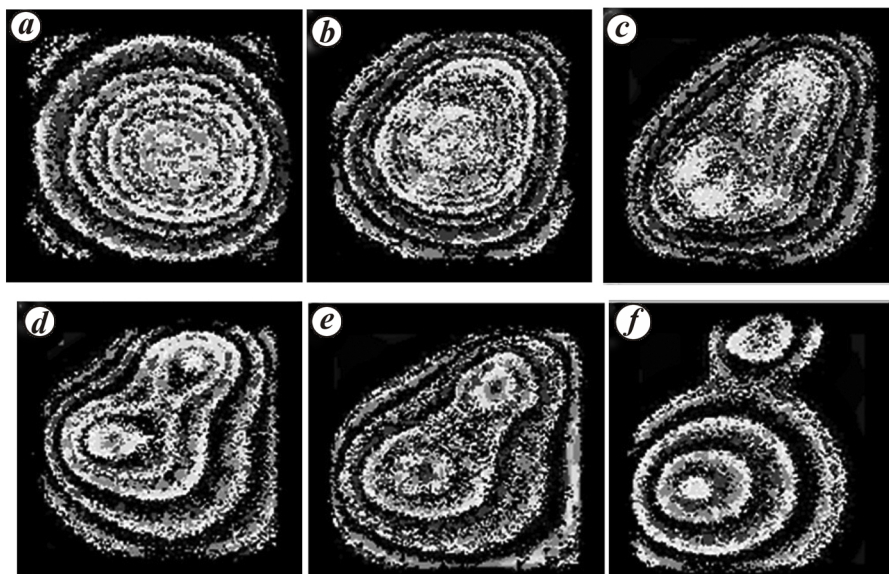


Figure 6. Images of Figure 5 after the step Filter > Pictorization > Monochrome Engraving in PhotoScape.

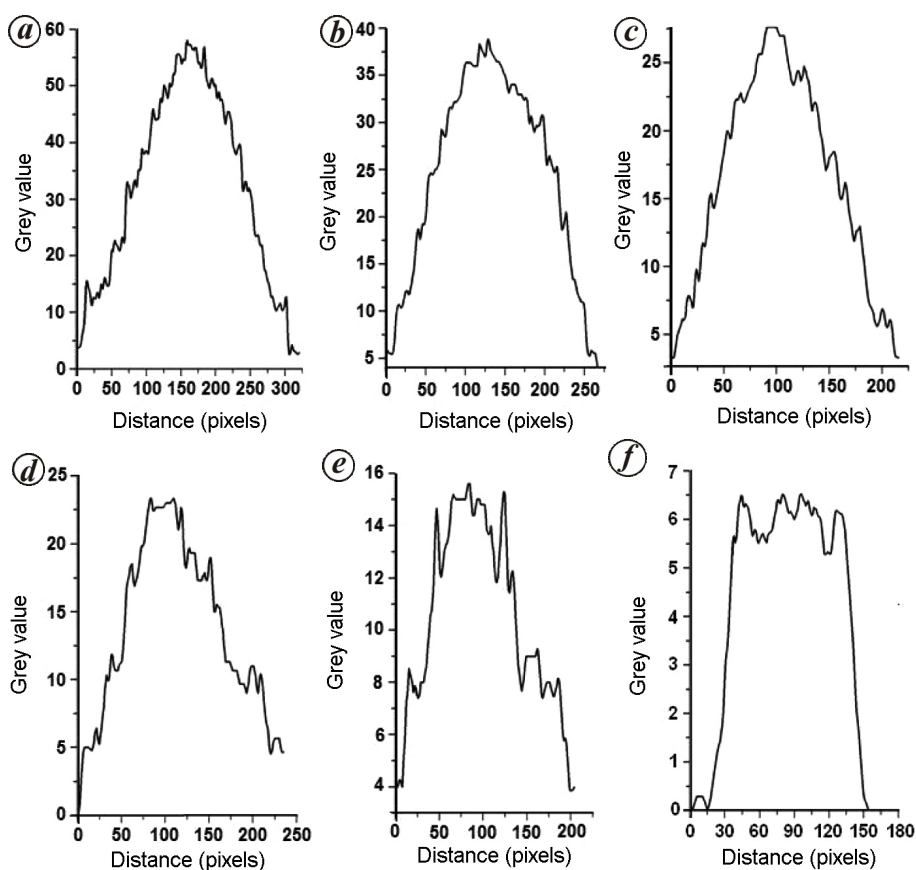


Figure 7. Intensity profiles for the interference fringes in Figure 5. *a*, For a difference in the optical path length of 2 cm, the maxima are quite clear. *b*, For an arm length difference of 4 cm, the contrast becomes a little poorer. *c*, *d*, For a differences of 6 and 8 cm respectively, two-point smoothing is done to ‘clean’ the plots. To avoid individual patterns of the two images, the area selected for plotting the intensity profile is between the two. Six and three maxima respectively, in both the rising and the falling halves of the profiles, are prominent. *e*, For a difference of 10 cm, three-point smoothing is done to make the maxima clear. Two maxima in each of the halves are visible. *f*, For a difference of 11.5 cm, eight-point smoothing is done to reduce the fluctuations. The fluctuations appearing in the constant-intensity region are the usual ones present in the beam, and consequently this length is considered as limiting one for the present experiment.

organ of the firefly has two segments of width approximately 1 mm separated by a few tens of micrometres, and these result in the appearance of interference rings in the two individual images. Clearly light from the two segments appears to be radiation from two different sources, and hence we have to consider the envelope of the two images for the measurement of temporal coherence. As the contrast of the rings in Figure 4*f* is very poor, we can consider this to be the limiting case. Its intensity profile in Figure 5*f* substantiates this fact. Hence, the coherence length for this light, more specifically yellow-coloured light, of the firefly is approximately $11.5 \times 2 = 23$ cm.

Random lasers typically exhibit low temporal coherence, roughly between 10 and 20 μm (refs 9 and 10). The coherence length for a typical Nd:YAG laser of wavelength 1.064 μm (FWHM = 0.45 nm) is just over 2 mm (ref. 11), and that for a pulsed one is normally in the order of a few centimetres¹². Compared to these values, the coherence length of 23 cm for this light of the firefly can be considered to be good. Recently, temporal coherence lengths of roughly the same order have been reported for a multimode narrow bandwidth tunable dye laser as 10 cm, for a multimode helium–neon laser of wavelength 632.8 nm as 19.20 cm, and for a copper vapour laser of wavelengths 510.6 and 578.2 nm as 4.3 and 2.7 cm respectively¹³.

As coherence length $l_c = c\tau_c$, c being the velocity of light, we have the coherence time $\tau_c = 7.66 \times 10^{-10}$ s. Taking the wavelength for the ‘monochromatic’ yellow radiation to be 591 nm (ref. 6), we have

$$\tau_c = \frac{\lambda^2}{c\delta\lambda},$$

or

$$\delta\lambda = \frac{\lambda^2}{c\tau_c} = 1.5 \times 10^{-3} \text{ nm}.$$

Hence we conclude that FWHM of the yellow line is $\sim 10^{-3}$ nm. This value is considerably narrower than many multimode solid state lasers. Random lasers exhibit broad emission spectra of bandwidth approximately 10 nm (ref. 9). A multimode free-running diode laser has a typical linewidth of 1 nm (ref. 14), and a 800 nm laser diode of this width would have a coherence length of about 0.64 mm (ref. 15).

In the Young double-slit method, interference fringes for pinhole separation of 160, 170 and 180 μm are shown in Figure 8*a–c* respectively, with their intensity profiles. As in the case of the Michelson interferometer, ‘noisy’ green and red emissions affect the contrast of the fringe. The visibility or contrast of the fringe is defined as

$$V = \frac{I_{\max} - I_{\min}}{I_{\max} + I_{\min}},$$

where I_{\max} is the maximum intensity at the centre of a bright interference fringe and I_{\min} is the minimum intensity at the centre of the adjoining dark fringe. The best central fringe visibilities for the present three cases are measured as 0.65, 0.56 and 0.39 respectively. These compare favourably with the intensity and visibility of spatial coherence fringes for random laser containing Rh6G and Al_2O_3 nanoparticles excited above the lasing threshold¹⁰, and also with a narrow bandwidth dye laser at a slit separation of 100 μm (ref. 13). Recently, it has been demonstrated that random lasers can be engineered to provide low spatial coherence¹⁶. In the present experiment, because of the faintness of the firefly emission, diameter of the pinholes had to be increased to 160 μm which, along with green and red emissions, definitely affect the contrast of the fringes. In spite of this, the fringes are reasonably good in appearance. In order to visualize the effects of green and red emissions on the contrast of the yellow rings, a close-up view of the central fringe is presented in Figure 6*d*, where bright rings representing interference maxima are visible.

To validate the work, we have used a commercial helium–neon laser of wavelength 632.8 nm. Figures 9 and 10 display the fringes obtained from this laser. In the Michelson interferometer, best contrast fringes for zero or no path difference, much poorer contrast fringes for 4.6 cm path difference and barely noticeable fringes for 9.5 cm path difference in the arms are shown in Figure 9*a–c* respectively. As the fringes disappear completely at

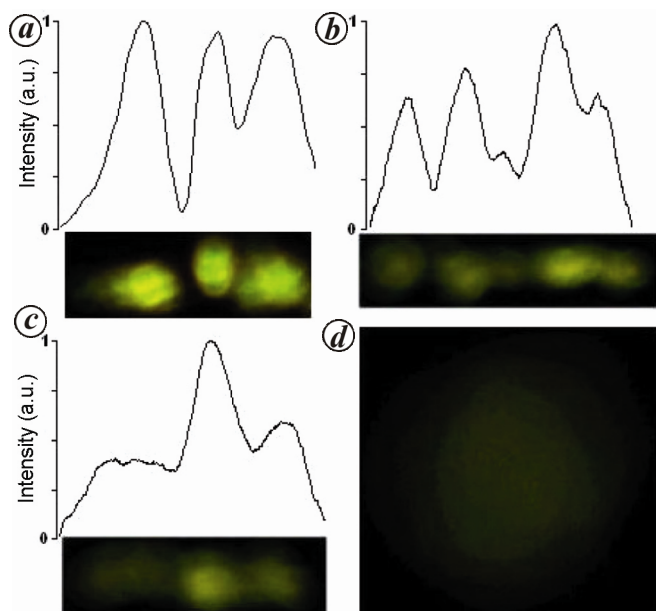


Figure 8. Interference patterns in the two-pinhole experiment for a hole diameter of 160 μm . *a*, For a hole separation of 160 μm , showing first-order fringes along with the central one. *b*, For a hole separation of 170 μm , presenting lower visibility. *c*, For a hole separation of 180 μm , showing a much lower contrast. *d*, Visualization of the effect of green and red sectors on the yellow sector: a close-up view of the central fringe recorded from a distance of 15 cm.

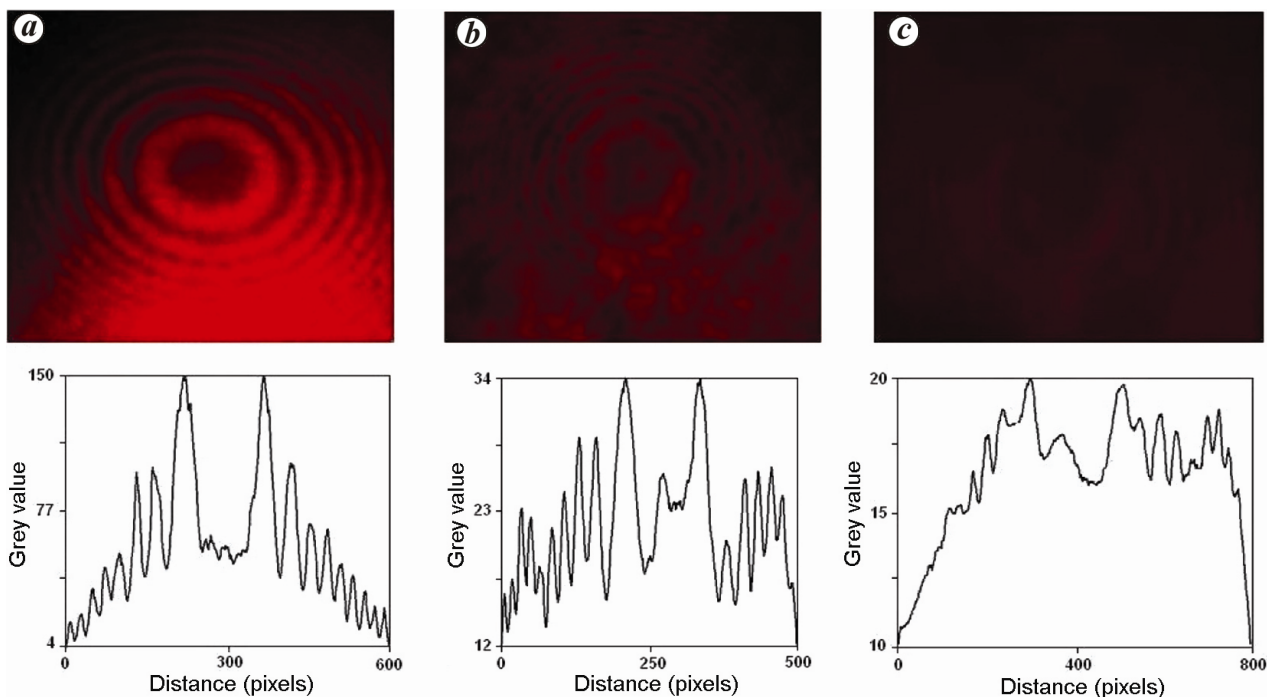


Figure 9. Fringes produced with the commercial multimode He–Ne laser in the Michelson interferometer. *a*, Zero path difference; *b*, 4.6 cm path difference; *c*, 9.5 cm path difference.

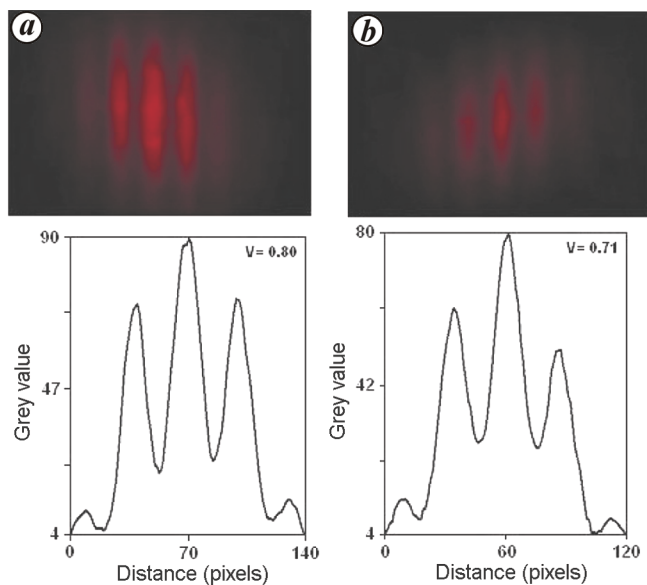


Figure 10. Fringes for the He–Ne laser in Young’s double-hole experiment. For pinhole separation of 160 μm (*a*) and 180 μm (*b*).

the path difference of 9.6 cm, the temporal coherence length for this laser radiation is 19.2 cm, which is also the value determined by Mensah *et al.*¹¹. Figure 10 displays the results of Young’s double-slit experiment for slit separation of 160 and 180 μm . Visibilities obtained in these cases are standard ones for this laser.

A mechanism for this highly coherent light has already been proposed⁶, which is discussed as follows. The firefly

light-emitting organ consists of a ventral photogenic layer and a dorsal reflector layer. The light reaction occurs in the photogenic layer, whereas the bioluminescence intensity is believed to be increased through reflection by the reflector layer, which is a specialized tissue. It has been reported that the cytosol of the reflector layer is filled with densely packed, opaque, spherical granules which should be uric acid granules, and that the reflector layer is about five times thicker than the photogenic layer; hence the assumption that the dense packing of tiny uric acid granules in a thick reflector layer does not allow the generated bioluminescent light to pass through the tissue¹⁷. Figure 11 shows an SEM image of these granules for *L. praeusta*. Diameters of these granules are of the order of the wavelength of the emitted light, and we have hypothesized that the emitted light waves are trapped by multiple scattering by them, implying that this disordered medium takes over the role of a regular laser cavity, similar to the one in the random laser. In a random laser, ring cavities formed by recurrent scattering have different loss, and the lasing frequency is determined by the cavity resonance. The possibility of generating random laser from a cell containing scattering particles in the cytosol, leading to a standalone cell laser has already been indicated¹⁸. It could be mentioned here that the bioluminescent spectrum of crude extract of luciferase from *L. praeusta* has similar emission maximum of 562 nm to the one observed in case of live fireflies, but most probably due to the absence of strong scattering no laser-like emission has been noticed¹⁹.

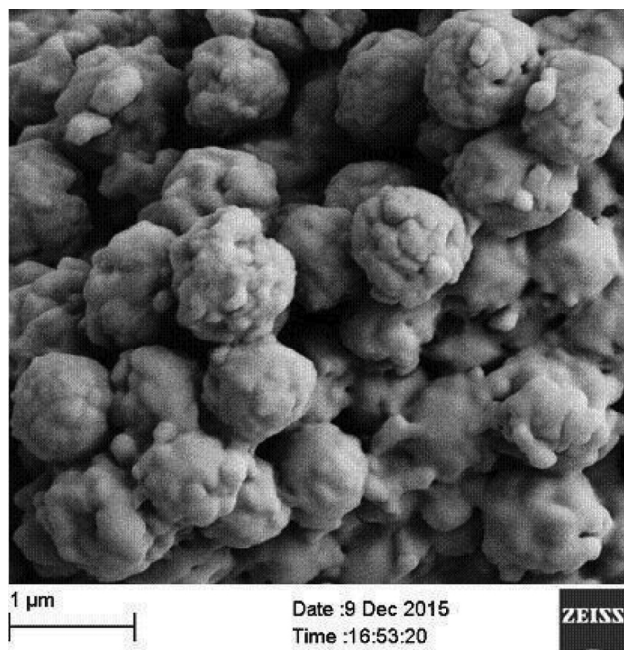


Figure 11. SEM image of uric acid granules in the reflector layer of the lantern of the Indian species of firefly *Luciola praeusta*.

In conclusion, the coherence length value of a couple of tens of centimetres for this species of the firefly is an astonishing one. This value quantifies as well as consolidates the laser-like emission detected in the emission spectrum of this species. The central fringe visibilities in the double-hole experiment suggest reasonably good spatial coherence. Hence an efficient laser system could be constructed in the model of the firefly light-emitting system. In firefly biology, there is definitely a scope for future studies in the role played by the high degree of coherence in communication – the yellow could possibly be the real coded signal. This work could be, and should be, extended to other species of fireflies to have a general idea on their coherence properties. In future, this should even be extended to other bioluminescent systems in the world.

6. Gohain Barua, A., Sharma, U., Phukan, M. and Hazarika, S., Sharp intense line in the bioluminescence emission of the firefly. *J. Biol. Phys.*, 2014, **40**, 267–274.
7. Goswami, A., Sharma, U., Rabha, M. M., Rajbongshi, S. C. and Gohain Barua, A., Steady-state and time-resolved bioluminescence of the firefly *Asymmetricata circumdata* (Motschulsky). *Curr. Sci.*, 2015, **109**, 1838–1842.
8. Wu, X., Chen, Q., Sun, Y. and Fan, X., Bio-inspired optofluidic lasers with luciferin. *Appl. Phys. Lett.*, 2013, **102**, 203706–1–3.
9. Papadakis, V. M., Andreas, S., Demetrios, A., Spiros, H. A., Giannelis, E. P. and Papazoglou, D. G., Single-shot temporal coherence measurements of random lasing media. *J. Opt. Soc. Am. B*, 2017, **24**, 31–36.
10. Ismail, W. Z. W., Liu, D., Clement, S., Coutts, D. W., Goldys, E. M. and Dawes, J. M., Spectral and coherence signatures of threshold in random lasers. *J. Opt.*, 2014, **16**, 105008.
11. Mensah, E. E., Pedersen, H. M. and Lokberg, A. J., Measurement of temporal coherence of visible cw laser sources using interferometric methods. *Afr. Rev. Phys.*, 2012, **7**, 433–439.
12. Raffel, M., Willert, C. and Kompenhans, J., *Particle Image Velocimetry*, Springer Verlag, Berlin, Heidelberg, New York, 1998, p. 29.
13. Singh, N. and Vora, H. S., On the coherence measurement of a narrow bandwidth dye laser. *Appl. Phys. B*, 2013, **110**, 483–489.
14. Samsøe, E. and Andersen, P. E., Improvement of spatial and temporal coherence of a broad area laser diode using an external-cavity design with double grating feedback. *Opt. Express*, 2014, **12**, 609–616.
15. www.worldoflasers.com/laserproperties.htm (accessed on 24 June 2015).
16. Redding, B., Choma, M. A. and Cao, H., Spatial coherence of random laser emission. *Opt. Lett.*, 2011, **36**, 3404–3406.
17. Goh, K. S., Sheu, H. S., Hua, T. E., Kang, M. H. and Li, C. W., Uric acid spherulites in the reflector layer of firefly light organ. *PLoS ONE*, 2013, **8**, e56406.
18. Fan, X. and Yun, S.-H., The potential of optofluidic biolasers. *Nature Methods*, 2014, **11**, 141–147.
19. Muthukumar, T., KrishnaMurthy, N. V., Sivaprasad, N. and Sudhaharan, T., Isolation and characterization of luciferase from Indian firefly *Luciola praeusta*. *Luminescence*, 2014, **29**, 20–28.

ACKNOWLEDGEMENTS. This work was supported by the University Grants Commission, New Delhi, Major Research Project F. No. 42-837/2013 (SR). We thank Mr M. M. Rabha, Pandit Deen Dayal Upadhyaya Adarsha Mahavidyalaya, Behali, Assam for help in the validation work.

Received 9 June 2017; revised accepted 25 September 2017

doi: 10.18520/cs/v114/i03/637-643

1. McElroy, W. D. and DeLuca, M., In *Bioluminescence in Action* (ed. Herring, P. J.), Academic Press, New York, 1978, pp. 109–127.
2. Ando, Y. *et al.*, Firefly bioluminescence quantum yield and colour change by pH sensitive green emission. *Nature Photonics*, 2008, **2**, 44–47.
3. Gohain Barua, A., Hazarika, S., Saikia, N. M. and Baruah, G. D., Bioluminescence emissions of the firefly *Luciola praeusta* Kiesenwetter 1874 (Coleoptera : Lampyridae : Luciolinae). *J. Biosci.*, 2009, **34**, 287–292.
4. Dehingia, N., Baruah, D., Siam, C., Gohain Barua, A. and Baruah, G. D., Purkinje effect and bioluminescence of fireflies. *Curr. Sci.*, 2010, **99**, 1425–1427.
5. Sharma, U., Phukan, M., Rabha, M. M. and Gohain Barua, A., Diffraction of the light of the firefly by a grating. *Astian J. Phys.*, 2014, **23**, 833–837.